International Journal of Energy Engineering 2012, 2(3): 67-72
DOI: 10.5923/j.ijee.20120203.02

Structural and Optical Characterization of Nitrogen-doped TiO_2 Thin Films Deposited by Spray Pyrolysis on Fluorine Doped Tin Oxide (FTO) Coated Glass Slides

C. O. Ayieko[1,*], **R. J. Musembi**[1], **S. M. Waita**[1], **B. O. Aduda**[1], **P. K. Jain**[2]

[1]Department of Physics, University of Nairobi, P.O. Box 00100, 30197, Nairobi, Kenya
[2]Department of Physics, University of Botswana, P/ Bag 0022, Gaborone, Botswana

Abstract Undoped and nitrogen-doped titanium dioxide (TiO2) thin films of 400 nm thick deposited by spray pyrolysis were structurally and optically characterized. The effect of substrate temperature on the optical properties of the films was also investigated. Structural studies of the films were undertaken by X-ray diffraction (XRD). Energy dispersive X-ray (EDX) spectrum analysis was used to confirm the presence of nitrogen atoms in the film after doping. The optical properties such as refractive index (n), energy band gap (Eg) and Urbach energy (Eu) were determined from spectrophotometric measurements of reflectance and transmittance for both undoped and doped films. The Undoped films had an energy band gap of 3.25 eV while the doped films had band gap of 2.90 eV. The Urbach energy increased from 1.00 eV for undoped films to 1.04 eV for the nitrogen-doped films. The reduction in energy band gap and increase in Urbach energy was attributed to the introduction of nitrogen impurity tail states on either the conduction band or the valence band of the titanium dioxide.

Keywords Titanium Dioxide, Spray Pyrolysis, Doping

1. Introduction

Titanium dioxide, TiO_2, has gained considerable attention because of its applications as a photocatalyst[1], solar cell electrodes[2] and gas sensors[3].

The structure and optical properties of TiO_2 depend to a large extend on the deposition technique. A number of techniques have been used to deposit TiO_2 films: direct current reactive magnetron sputtering and thermal annealing method[4], pressing method[5] and dip coating[6]. Another method of influencing the properties of TiO_2 films is by doping with elements like indium (In) and chromium (Cr)[7] cadmium (Cd), cesium (Ce) and iron (Fe)[8] on TiO_2 films obtained by r.f sputtering.

Apart from metallic dopants, non metallic dopant like Nitrogen (N_2) gas has also been used to influence the properties of TiO_2 films and an increase in visible light absorption of TiO_2 after N_2 doping[9]. The effect of doping TiO_2 with N_2 gas on the optical properties of TiO_2 for dye sensitized solar cells applications has also been studied[4] where increased film transmittance and higher photoresponse in the visible spectrum was observed.

Not much information is available for N_2-doped spray deposited TiO_2 films. This paper reports on the structural and optical properties of N_2-doped TiO_2 films deposited by the spray pyrolysis technique and investigates the widening the spectral limit of solar radiation through increased absorption.

2. Experimental

Microscope glass slides (MGS) as well as fluorine doped tin oxide coated glass substrates (FTO) were used and were cleaned before deposition by keeping them in an ultrasonic bath filled with distilled water for 2 minutes. The substrates were then kept in acetone for 20 minutes and finally rinsed in distilled water. MGS were used as control to see if the nature of substrates affects the optical properties of TiO_2.

For the deposition TiO_2 by spray pyrolysis, 120 µl of commercially available titanium (iv) isopropoxide ($TiC_{12}H_{28}O_4$) (99.7% pure) and 200 ml isopropanol (C_3H_8O) (99.7% pure) from Fluka Ltd were mixed in a 500 ml beaker. The mixture was maintained at a temperature of 50 °C using an electric hot plate while stirring with a magnetic stirrer for about 15 minutes. This mixture formed the precursor which was atomized by the spray system using compressed

---

* Corresponding author:
opiyoc2006@yahoo.com (C. O. Ayieko)

nitrogen as the carrier gas.

The spray nozzle-to-substrate distance was set to about 15 cm. The substrate temperature was set to 200 °C, 150 °C and 100 °C for different samples. Spraying was done in pulses. A pulse consisted of 5 seconds of spraying and 30 seconds of pause. Ten pulses were done for every sample at a precursor flow rate of 2.6 ml/min. The chemical reaction resulting in the formation of amorphous TiO_2 thin film was as follows;

$$TiC_{12}H_{28}O_{4(aq)} + 17O_{2(g)} + 2C_3H_8O_{(aq)}\ \mathit{T_s(100^oC\text{-}200^oC)} \longrightarrow TiO_{2(s)}(\text{amorph}) + 8CO_{2(g)} + H_2O_{(g)} \tag{1}$$

$$TiO_{2\,(s)}\ (\text{amorph})\ \textit{annealing (30 min) at 400 }^o\textit{C} \longrightarrow TiO_{2\,(s)}\ (\text{polycrystalline}) \tag{2}$$

The film thicknesses were determined using a computerized KLA-Tencor Alpha –Step IQ surface profiler.

For nitrogen doping, a pyrex glass tube placed in a programmable horizontal tube furnace (ThermoScientific Lindberg/Blue Mini-Mite) was used for heating the samples in nitrogen gas atmosphere. The tube furnace was fitted with a digital themometer which was used to measure the temperature of the samples' chamber. Samples were loaded into the chamber using a metallic sample holder and heated gradually from room temperature upto a fixed temperature of 450 °C.

Nitrogen gas flow into the chamber was maintained at the rate of 20 cm^3/sec via Labview Inc. Computer software that interfaced with digital flowmeter connected to a nitrogen gas cylinder. After 30 minutes the samples were allowed to cool to room temperature without cutting off nitrogen flow.

The structure of the films was characterized by X-ray diffraction (XRD) using a Phillips, PW 3710 XRD machine interfaced with computer installed with Analytical X'Pert 2000 data collection software. EDX studies were carried out using scanning electron microscope (SEM) model Phillips, XL 30 ESEM, integrated with energy dispersive X-ray unit (EDX). The SEM micrographs for the study of surface morphology were obtained by examination using Carl Zeiss^{TM} LEO 1530 SEM model.

Total transmittance and reflectance measurements were taken at near normal incidence in the wavelength range of 300-1200 nm using a computerized double beam solid-spec 3700 DUV Shimadzu Spectrophotometer equipped with 198851 Barium Sulphate ($BaSO_4$) integrating sphere. The reflectance and transmittance data were used for calculation of optical properties such as band gap, Urbach energy and refractive index.

3. Results and Discussion

3.1. Structural Analysis

Figure 1 shows the X-ray diffraction (XRD) pattern of TiO_2 thin films deposited on FTO substrates at a substrate temperature of 200 °C. The films were amorphous but when annealed at 400 °C in air, distinct peaks of (101), (112) and (204) orientation formed showing crystallization. Our results are in agreement with the findings of other researchers who have obtained an amorphous-crystalline transition temperature of ~ 350 °C for TiO_2[4]. The SnO_2 peaks are from the FTO glass substrate.

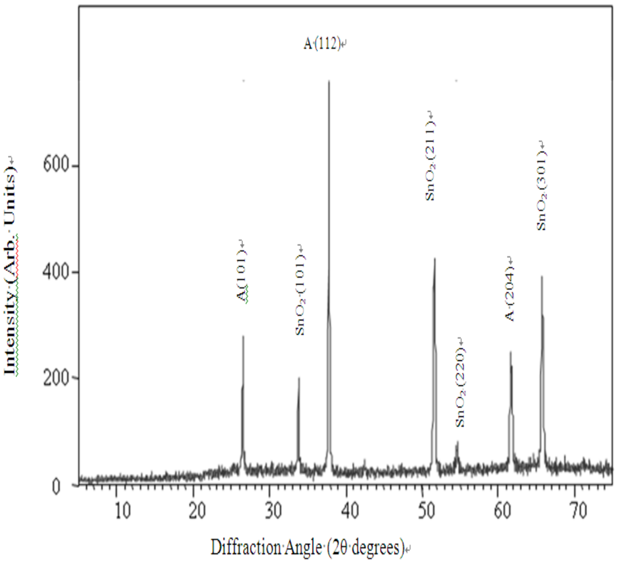

Figure 1. XRD-pattern for TiO_2 film deposited on FTO glass at a substrate temperature of 200 °C and annealed at 400 °C (A – anatase, SnO_2 - tin oxide).

3.2. Optical Characterization

3.2.1. Reflectance and Transmittance

Figure 2 shows absorption coefficient, α, of the various samples of nitrogen doped and undoped TiO_2 thin films both annealed and unannealed and it is observed that at all wavelengths the absorption coefficient, α, is higher for the nitrogen-doped films compared to the undoped films. This means that within the wavelength range of 300 – 1200 nm considered there is enhanced absorption. Figure 3 shows transmittance and reflectance properties for undoped and nitrogen-doped samples both annealed and unannealed.

Absorption, reflectance and transmittance should all add up to unity. Notable from Fig.3 is that the transmittance of the undoped films is higher for the doped for all wavelengths, but reflectance is fairly constant. This implies that only transmittance and absorptance of the film vary. Therefore if transmittance is high then absorption is reduced and vice versa and therefore we can infer from both figures (Fig.2 and Fig.3) that doping increases absorptance.

The graphs in Fig.2 and Fig.3 shifts towards the right, that is, from ultra violet region to visible region on doping the films whether annealed or unannealed. This is indicative of an improvement in photo-absorption. This improvement is attributed to the reduction of band gap upon nitrogen doping. Considering the graphs for the doped samples in Figure 2 it is noted that absorption coefficients are higher for the doped TiO_2 thin films within the visible part of the spectrum. The enhanced absorption is due to nitrogen doping which increases the absorption coefficient of the film.

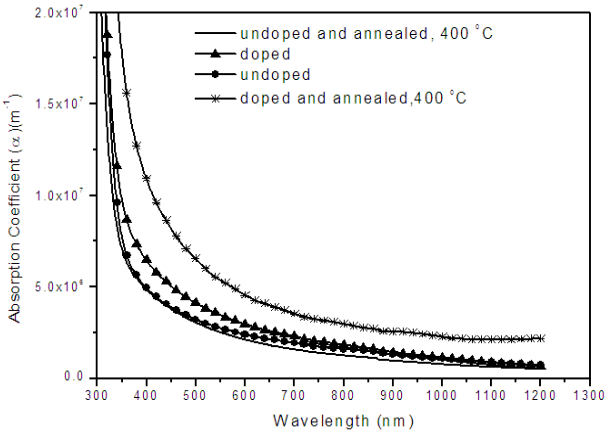

Figure 2. Dependence of absorption co-efficient on the wavelength of nitrogen - doped and undoped TiO_2 thin film of thickness of 400 nm deposited on Flourine doped tin oxide (FTO) glass slides.

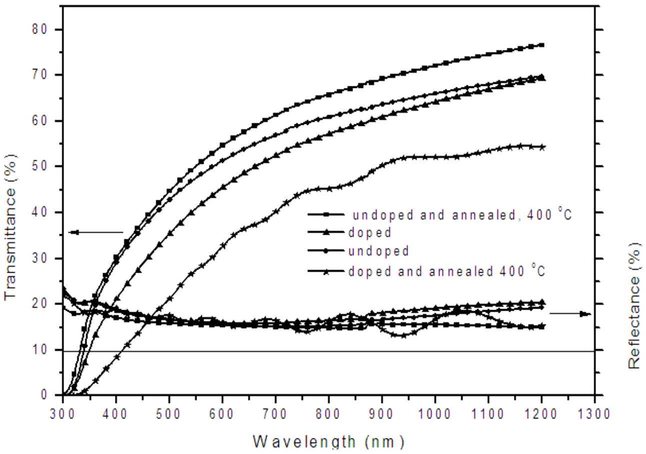

Figure 3. Dependence of transmittance and reflectance on the wavelength of nitrogen - doped and undoped TiO_2 thin film of 400 nm thickness deposited on (FTO) glass slid.

From Fig. 3 reflectance curves cluster in a narrow range for the wavelength range considered here as opposed to transmittance that varies greatly with the sample treatment. The nitrogen-doped sample records the lowest transmittance across the considered spectrum. This shows that the nitrogen-doped sample has high absorption for the wavelength range presented.

To establish the part of the spectrum where enhanced photoresponse is evident due to nitrogen doping, equation (3) is used[10]:

$$E_\lambda = \frac{1.24}{\lambda(\mu m)} \tag{3}$$

where the E_λ is energy in eV and λ is wavelength in micrometers (μm). The equation gives wavelengths which correspond to a minimum of 428 nm and a maximum of 384 nm that is also confirmed by the observation of band gap reduction due to doping in Section 3.2.4. This is very remarkable since nitrogen doping enhance light absorption beyond the visible to near infra-red.

3.2.2. Refractive Index

The wavelength dependence of refractive index of the film formed at different substrate temperatures (T_s) was calculated from reflectance data using eq (4)[11]:

$$n = \frac{1+R}{1-R} + \sqrt{\frac{4R}{(1-R)^2} - K^2} \tag{4}$$

where n is the refractive index, R is the reflectance and K is the extinction co-efficient.

The refractive index, n, of annealed and unannealed TiO_2 films deposited at different substrate temperatures is shown in Fig. 4. The refractive index, n, shows a general decrease as the wavelength increases for all the substrate temperatures (T_s). The graphs are typical of normal dispersion where refractive index reduces with increase in wavelength due to electronic inter-band absorption for photon energies greater than the smallest band gap in the ultra-violet region which extends to the visible region[11].

It is clear from Fig. 4 that refractive index increases with substrate temperature, an observation that concurs with the findings[12]. This increase is attributed to annihilation of pores since the film surface gets denser as the temperature of the substrate increases. This is because a denser material has a larger refractive index since more electric dipoles are activated when the material is exposed to electric field of the incoming light radiation[11].

Kumagai *et. al* employed Cauchy-Rieman's dispersion law (eqn. 5) to study refractive index of amorphous TiO_2 thin film deposited by controlled growth with sequential surface chemical reactions[13];

$$n(\lambda) = A_n + B_n/\lambda^2 + C_n/\lambda^4 \ (\lambda \text{ in } \mu\text{m}) \tag{5}$$

where A_n, B_n and C_n are fitting coefficients specific to material in consideration. The values obtained for A_n, B_n and C_n were 2.2100, 0.0240 and 0.0011 respectively in the wavelength range of 300 – 800 nm[13]. Having fed the above fitting parameters in Cauchy-Rieman's dispersion law as verification of our results, we obtained the curves in Fig. 4 with the exemption of the curve for $T_s = 400^oC$ (crystalline TiO_2).

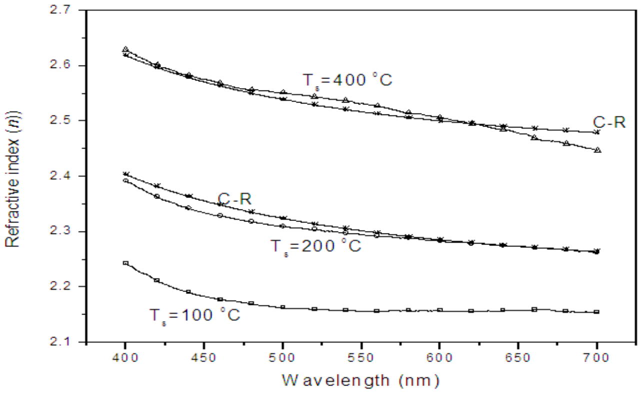

Figure 4. Effect of substrate temperature and annealing on refractive index of TiO_2 coated on MGS at 100 °C and 200 °C and Cauchy Rieman dispersion law. C-R – Cauchy Rieman's Curve.

It is observed that our results conform to the Cauchy-Rieman's dispersion law in the general trend of variation of the refractive index, *n*, with wavelength, *λ*. Furthermore, the films deposited at 200 °C are in very good agreement with the Cauchy-Rieman's dispersion law especially at longer wavelengths (600 - 700 nm). This agreement can be traced to the amorphous nature of both our films and Cauchy-Rieman's. The deviation at wavelengths less than 600 nm may be accounted for by the errors in computing A_n and B_n respectively[13].

However, the dispersion curve for crystalline sample (sample prepared at 200 °C annealed at 400 °C) did not fit very well onto the Cauchy-Rieman's curve as shown in the Fig. 4. Using the fitting tool in Origin Inc. Software the fitting coefficients A_n, B_n and C_n for the annealed sample had values of 2.4350, 0.0240 and 0.0011 respectively within the wavelength range of 300 – 800 nm for the crystalline samples. The difference in the fitting coefficients for the crystalline samples compared to the amorphous samples was only in the first term which does not involve the wavelengths.

The fitting coefficients B_n and C_n which involve the terms associated with wavelength come into play at longer wavelengths for crystalline samples where we see a small deviation especially above 650 nm. The difference in the fitting coefficients for the samples deposited at 200 °C (unannealed) and samples annealed at 400 °C is due to the change in phase from amorphous to crystalline structures upon annealing as shown by XRD results (Fig. 1).

Because of poor adherence on the substrates of films deposited at temperatures below 200 °C and in this case 100 °C, Cauchy's curve was not presented but the refractive index curve is presented to show the effect of substrate temperature.

3.2.3. Effect of Substrate Temperature and Nature of Substrate on Band Gap

Figure 5 shows a plot of $(\alpha h\nu)^2$ versus *hv* for the determination of band gap for film grown on both MGS and FTO glass substrates. The band gap values are given in Table 1. It is noted that within the experimental error (± 0.08 eV) the band gap is invariant with substrate temperature. for film grown on both MGS and FTO glass substrates as shown in Table 1.

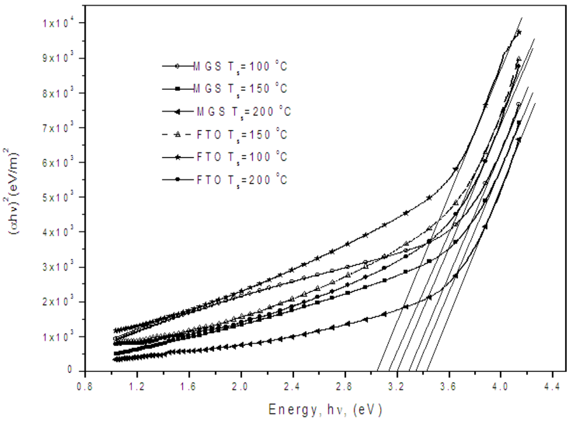

Figure 5. A plot of $(\alpha h\nu)^2$ vs *hv* for determination of band gap.

Table 1. Variation of band gap with temperature and nature of the substrate.

	Substrate temperature, T_s = 100 °C	Substrate temperature, T_s = 150 °C	Substrate temperature, T_s = 200 °C
Band gap (± 0.08 eV) (FTOsubstrates)	3.15	3.18	3.20
Band gap (± 0.08 eV) (MGS substrates)	3.25	3.30	3.40

The band gaps of TiO_2 thin film coated on MGS was observed to be higher than the band gaps recorded for TiO_2 thin film coated on FTO for all cases of substrate temperatures, which can be accounted for from the fact that the coating on FTO substrates is a combination of TiO_2 thin film and fluorine doped tin oxide resulting in effectively a much thicker film(s) compared to the one(s) coated on MGS substrates. This increase in thickness increases the absorptance values for TiO_2 thin film coated on FTO substrates. When the band gap (E_g) is made the subject of the formula in the following equation[8];

$$\alpha h\nu = a\left(h\nu - E_g\right)^r \quad (6)$$

(where *α* is the absorption coefficient, *a* is a constant that does not depend on the photon energy and *r* is the numerical constant which has the value of ½), the band gap (E_g) varies as the square of absorptance (α^2) and the term involving α^2 is subtracted from a constant values hence reducing the band gap. This justifies the low band gap values for TiO_2 thin film coated on FTO substrates whose absorptance are higher.

Despite the difference in band gaps of TiO_2 coated on FTO and MGS, band gap values as shown in Fig. 5 are still within the range of 3.10 - 3.40 eV as observed in the previous studies for the as prepared TiO_2 films[14].

3.2.4. Effect of Nitrogen-Doping On the Band Gap of TiO_2 Coated on Fluorine Doped Tin Oxide (FTO) Glass Slides

Figure 6 presents the band gaps of films coated on fluorine doped tin oxide (FTO) substrate and annealed at 400 °C. There was a significant decrease in the band gap, the undoped film had a band gap of 3.25 eV compared to the nitrogen-doped which had 2.90 eV. This observation concurs with results earlier obtained by Baoshun[15] who also observed a significant decrease in the band gap TiO_2 prepared by sputtering from 3.2 eV to 2.7 eV upon nitrogen doping. This reduction is as a result of nitrogen impurity states which introduce tail energy levels either in the conduction band or valence or both of the undoped titanium dioxide.

The presence of nitrogen in the structure of TiO_2 is further confirmed by EDX results shown in Fig.7. The more pronounced peak is that of oxygen which is a combination of the oxygen in fluorine-doped tin oxide ($F:SnO_2$) back contact and TiO_2. Since carbon paste was used to make the films conductive in SEM analysis, the carbon peak observed could be from the paste but not the film coating and hence not forming part of the intended film. The peaks for titanium were not seen since the appearance of an element in the micrograph depends upon its electronic configuration and the acceleration voltage which in certain ranges only elements with given atomic numbers can be detected.

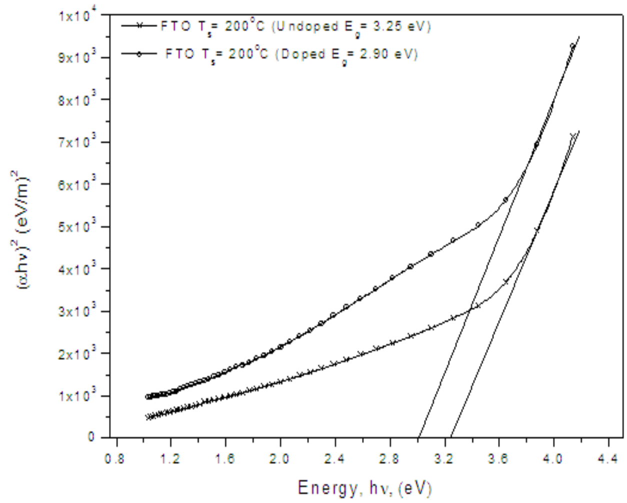

Figure 6. Graph showing the effect of doping TiO_2 thin film coated on conducting flourine doped tin oxide (FTO) glass slides with nitrogen (N_2) and annealed at 400 °C.

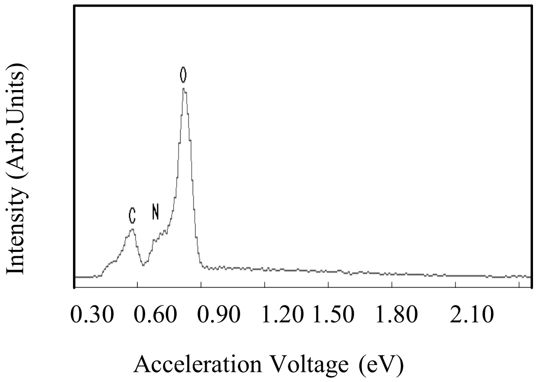

Figure 7. EDX micrograph of the nitrogen–doped TiO_2 (N: TiO_2) coating on FTO glass substrates annealed at 400 °C in air.

3.3. Urbach Energy

Modification of the band structure which may be due to introduction of defects in a material can be established by determining the materials Urbach energy before and after the defects are introduced. Urbach energy gives a measure of structural disorder in a material. The formula for determination of Urbach energy is as follows[7]:

$$(\alpha h\nu) = \alpha_o \exp\left(\frac{h\nu}{E_u}\right) \tag{7}$$

Urbach energy was determined for N_2-doped and undoped TiO_2 thin films as shown in Fig. 8. The Urbach energy of the undoped film on conducting glass (FTO) is 1.000 eV ± 1.3% while the Nitrogen-doped film has Urbach energy of 1.041 eV ± 1.3%. The difference in Urbach energy is because of the impurity levels introduced by doping in the band structure of undoped films. Since higher Urbach energy is indicative of considerable introduction of tail states at the band edges, the higher E_u value for nitrogen-doped film confirms further introduction of tail states compared to the undoped films.

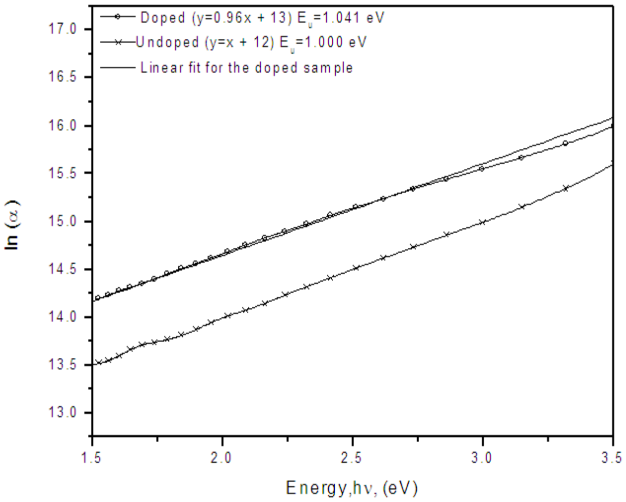

Figure 8. Urbach energy (E_u) of nitrogen doped and undoped TiO_2 coated on conducting flourine doped tin oxide (FTO) glass slides.

4. Conclusions

TiO_2 thin film deposited by spray pyrolysis at substrate temperature of 100 °C is amorphous but when annealed at 400 °C, it changes phase to anatase with sharp XRD peaks showing crystallization as temperature increases. XRD studies showed that after annealing the films were predominantly anatase with characteristic (101), (112) and (204) planes.

Optical studies were carried out on the nitrogen-doped and undoped TiO_2 films and reflectance, transmittance, band gap, refractive index and Urbach energy were determined. From the transmittance and reflectance spectra, nitrogen-doped films had higher absorption compared to the undoped films. The energy band gap of titanium dioxide (TiO_2) was not affected by substrate temperature if coated by spray pyrolysis on same substrate material, however, if the nature of the substrate material was changed the energy band gap changed slightly. The values of the energy band gap obtained fall between 3.10 eV to 3.4 eV which was within the range of values for TiO_2 phases, that is approximately 3.2 eV recorded upon annealing. Refractive index, *n*, of TiO_2 film was established to increase with substrate temperature due to densification of the films as the temperature increases. The refractive index shows a general decrease as the wavelength increases for all the substrate temperatures.

Doping the TiO_2 thin film with nitrogen reduces the band gap but increases Urbach energy both is attributed to the introduction of impurity states either on the conduction band or valence or both conduction and valence bands. There was a significant decrease in the band gap upon doping, the undoped film had a band gap of 3.25 eV compared to the nitrogen-doped which had 2.90 eV. The Urbach energy increased from 1.000 eV for undoped films to 1.041 eV for nitrogen-doped films.

ACKNOWLEDGEMENTS

This work is supported by African Materials Science and Engineering Network (AMSEN) and International Programme in the Physical Sciences (IPPS), Uppsala University (Sweden).

REFERENCES

[1] Abou-Helal, M. O. and W.T. Seeber (2002), Preparation of TiO_2 thin films by spray pyrolysis to be used as photocatalyst, Applied Surface Science 195, 53.

[2] Gratzel, M and B. O'Regan (1991), Low cost, high efficiency cell based on dye-sensitized colloidal TiO_2 films, Nature 353, 737-740.

[3] Castaneda, L., J. C. Alonso, A. Ortiz, E. Andrade, J. M. Saniger, J. G. Banuelos (2002). Spray pyrolysis deposition and characterization of titanium dioxide thin films, Material chemical physics 77, 938.

[4] Waita, S. M., B. O. Aduda, J. M. Mwabora, C. G. Granqvist, S. Lindquist, G. A. Niklasson, A. Hagfeldt, G. Boschloo (2007). Electron transport and recombination in dye sensitized solar cells fabricated from obliquely sputter deposited and thermally annealed TiO2 films. Journal of Electroanalytical Chemistry 605, 151–156.

[5] Wafula, B., J. Simiyu, S. Waita, B. Aduda, J. Mwabora (2007). Effect of nitration on pressed TiO_2 Photoelectrodes for Dye-Sensitized solar cells, African Journal of Science and Technology (AJST), Science and Engineering Series 8, (2) 63-71.

[6] Hemissi, M., H. A. Adnani, J. C. Plenet (2009). Titanium dioxide thin layers deposited by dip-coating method, their optical and structural properties. Current Applied Physics, 9, 717-721.

[7] Arushanov, E., S. Levcenko, N. Syrbu, V.Tezlevan, M. Merino, M.Leon (2006). Urbach's tail in the absorption Spectra of $CuIn_5S_8$ and $CuGa_3Se_5$ Single crystals, Phys. Sta. Sol (a) 203, (11) 2909-2912.

[8] Mardare, D., M. Tasca, M. Delibas, G.I. Rusu(2000). On the structural properties and optical transmittance of r.f sputtered films. Applied Surface Science 156, 200-206.

[9] Torbjon, L., J. M. Mwabora, E. Avendan˜ o, J. Jonsson, A. Hoel, C. Granqvist, S. Lindquist (2003). Photoelectrochemical and Optical Properties of Nitrogen Doped Titanium Dioxide Films Prepared by Reactive DC Magnetron Sputtering J. Phys. Chem. B, 107, 5709-5716.

[10] Anderson, D. (2001). Clean Electricity from Photovoltaics, M.D Archer and R.D. Hill Edition, Imperial College Press: London.Hemissi, M., H. A. Adnani, J. C. Plenet (2009). Titanium dioxide thin layers deposited by dip-coating method, their optical and structural properties. Current Applied Physics, 9, 717-721

[11] Aksay, S. and B. Altiokka (2007). Effect of substrate temperature on some of the optical parameters of $CuInS_2$ films, Phys. Sta. Sol. (c) 4, (2) 585-588.

[12] Hassan, M.M., A.S.M.A. Haseeb, R. Saidur, H.H. Masjuki (2008). Effects of annealing treatment on optical properties of anatase TiO_2 thin films. International Journal of Chemical and Bimolecular Engineering 1:2www.waset.org Spring (93-97).

[13] Kumagai, H., M. Matsumoto, K. Toyoda, M. Obara, M. Suzuki (1995). Fabrication of titanium oxide thin films by controlled growth with sequential surface chemical reactions, Thin Solid Films 263, 47-53.

[14] Ali, H. (2005). Characterization of a new transparent-Conducting material of ZnO doped ITO films, Phys.Sta.Sol (a) 202, (14) 2742-2752.

[15] Baoshun, L., W. Liping, Z. Xiujian (2007). The structure and photocatalytic studies of N-doped TiO_2 films prepared by radio frequency reactive magnetron sputtering. Solar Energy Materials and Solar Cells, 92, 1-10.